Journal of Colloid and Interface Science **218,** 289–299 (1999)
Article ID jcis.1999.6405, available online at http://www.idealibrary.com on IDEAL®

An *in Situ* ATR-FTIR Investigation of Sulfate Bonding Mechanisms on Goethite

Derek Peak,[1] Robert G. Ford,[2] and Donald L. Sparks

Department of Plant and Soil Sciences, University of Delaware, 149 Townsend Hall, Newark, Delaware 19717-1303

Received March 10, 1999; accepted July 6, 1999

The mechanism of sulfate adsorption on goethite was investigated *in situ* using attenuated total reflectance Fourier transform infrared (ATR-FTIR) spectroscopy. Sulfate adsorption was investigated at ionic strengths between 0.005 and 0.1 M, reactant concentrations between 5 and 500 μM, and pH values between 3.5 and 9.0. It was determined that sulfate forms both outer-sphere and inner-sphere surface complexes on goethite at pH less than 6. At pH values greater than 6, sulfate adsorbs on goethite only as an outer-sphere complex. The relative amount of outer-sphere sulfate surface complexation increased with decreasing ionic strength. The spectrum of sulfate adsorbed on goethite was also compared to the infrared spectrum of synthetic schwertmannite, an iron(III) oxy-hydroxy-sulfate. It was determined that *in situ* spectra of both schwertmannite and adsorbed sulfate are quite similar, suggesting that a continuum of outer- and inner-sphere sulfate occurs in both cases.

Key Words: **sulfate; surface complexation; ATR-FTIR; goethite; bonding mechanisms; *in situ* spectroscopy; schwertmannite.**

INTRODUCTION

Sulfate is an oxyanion that is commonly found in the soil environment. It occurs in extremely high concentrations near acid mine runoff and is produced as a result of the geochemical cycling of pyrite (1). Sulfate is of environmental importance for several reasons. It can affect the availability of trace metals by enhancing metal sorption at lower pH (2, 3). Sulfate adsorption also competes to some extent with the sorption of other anions such as phosphate (4) and low molecular weight organic acids (5). To accurately predict the interactions of sulfate with colloid interfaces, a thorough understanding of sulfate adsorption mechanisms on soil components is needed.

Macroscopic experiments of sulfate sorption have provided results that are consistent with an outer-sphere (electrostatic) adsorption mechanism on both soils and reference minerals (6). This conclusion is supported primarily by two observations. (i) Ionic strength has a large effect on the amount of sulfate that is adsorbed, with increasing adsorption as the ionic strength decreases. (ii) No adsorption of sulfate is usually seen above the point of zero charge (PZC) of the mineral. This fact potentially makes iron and aluminum oxides important sites for sulfate adsorption in soils since these components have high points of zero charge and are commonly found in soils. Zhang and Sparks (7) conducted pressure-jump relaxation studies of sulfate adsorption on goethite and determined that the reaction kinetics could be described well with outer-sphere complexation accompanied with simultaneous surface site protonation.

Sposito (8) suggested that sulfate adsorption might be of an intermediate nature, sometimes sorbing as an outer-sphere complex and sometimes as an inner-sphere complex via a ligand exchange mechanism. This concept was supported by the observations of Yates and Healy (9) who investigated sulfate adsorption on both α-FeOOH and α-Cr_2O_3. Although the rates of hydroxyl exchange for the two sorbents are markedly different, the rate and extent of sulfate adsorption was very similar, implying an outer-sphere complexation mechanism. However, sulfate adsorption also shifts the point of zero charge to higher values on both α-FeOOH and α-Cr_2O_3, which is consistent with inner-sphere complexation.

It is important to realize that sorption mechanisms can not be conclusively determined with macroscopic experiments alone. Spectroscopic methods are necessary to verify conclusions drawn from macroscopic observation (10). Although somewhat contradictory to the macroscopic laboratory studies, there is microscopic and spectroscopic evidence of sulfate inner-sphere surface complexation. Transmission infrared spectroscopic studies of sulfate adsorption on goethite and hematite (11, 12) revealed the formation of sulfate bidentate binuclear surface complexes on both solids. More recently, Persson and Lövgren (13) concluded that outer-sphere adsorption of sulfate on goethite was occurring on the basis of results from diffuse reflectance infrared (DRIFT) spectroscopy. However, these spectroscopic experiments all involved potential sample alteration via either drying, the application of heat and pressure, or dilution in a salt which could have modified the structure of the original sorption complex.

It is greatly preferable to conduct *in situ* experimentation to elucidate interactions that occur in aqueous suspensions. *In situ* experiments using scanning tunneling microscopy (STM) (14)

[1] To whom correspondence should be addressed. E-mail: dpeak@udel.edu.
[2] Current address: United States EPA, Kerr Environmental Research Center, P.O. Box 1198, Ada Oklahoma 74820.

0021-9797/99 $30.00

and ATR-FTIR spectroscopy (14, 15) to determine the adsorption mechanism of sulfate on hematite have more recently shown that inner-sphere monodentate surface complexes form at the hematite surface under aqueous conditions.

It was the goal of this research to thoroughly investigate the adsorption mechanism of sulfate on goethite using an *in situ* technique and attempt to reconcile the differences between previous macroscopic and spectroscopic studies in the literature. While macroscopic experiments (6) have revealed a strong ionic strength influence on sulfate adsorption, the effect of ionic strength on sulfate surface complexation mechanisms has not been investigated using *in situ* spectroscopy. Goethite was chosen as a sorbent because it is the most common iron oxide found in soils (16) and its structure is stable over a wide pH range. *In situ* (ATR-FTIR) spectroscopy was employed, since sulfate absorbance is well resolved from goethite absorbance in the mid-infrared region. Schwertmannite was used as a reference phase since this iron oxide contains sulfate in both outer-sphere and inner-sphere coordination environments (1).

Infrared Theory

The relationship between the symmetry of sulfate complexes and their infrared spectra is well established (17), and it is possible to assign molecular symmetry based on the number and position of peaks that appear in the mid-infrared region. With the ATR technique under aqueous conditions, there are two infrared sulfate vibrations that are accessible to spectroscopic investigation. They are the nondegenerate symmetric stretching v_1 and the triply degenerate asymmetric stretching v_3 bands (13). As a free anion in solution, sulfate has tetrahedral symmetry and belongs to the point group T_d. For this symmetry, only one broad peak at approximately 1100 cm^{-1} due to the triply degenerate vv_3 band is usually observed. In some cases the v_1 band is also weakly active and appears at around 975 cm^{-1}. Since outer-sphere complexes retain their waters of hydration and form no surface chemical bonds, it can be expected that the symmetry of outer-sphere sulfate complexes would be similar to aqueous sulfate. However, distortion due to electrostatic effects could shift the v_3 to higher wavenumber and cause the v_1 band to become IR active. If sulfate is present as an inner-sphere complex, the symmetry is lowered. As a result, the v_1 band becomes infrared active and the v_3 band splits into more than one peak. In the case of a monodentate inner-sphere surface complex, such as that observed for sulfate adsorption on hematite, C_{3v} symmetry results. The v_3 band splits into two peaks, one at higher wavenumber and one at lower wavenumber, while the v_1 band becomes fully active at about 975 cm^{-1} (15, 17). If sulfate forms a bidentate binuclear (bridging) surface complex, the symmetry is further lowered to C_{2v}, and the v_3 band splits into three bands between 1050 and 1250 cm^{-1}, while the v_1 band is shifted to around 1000 cm^{-1} (17). The relationship between the symmetry of surface complexes and the resulting infrared spectrum is summarized in Fig. 1.

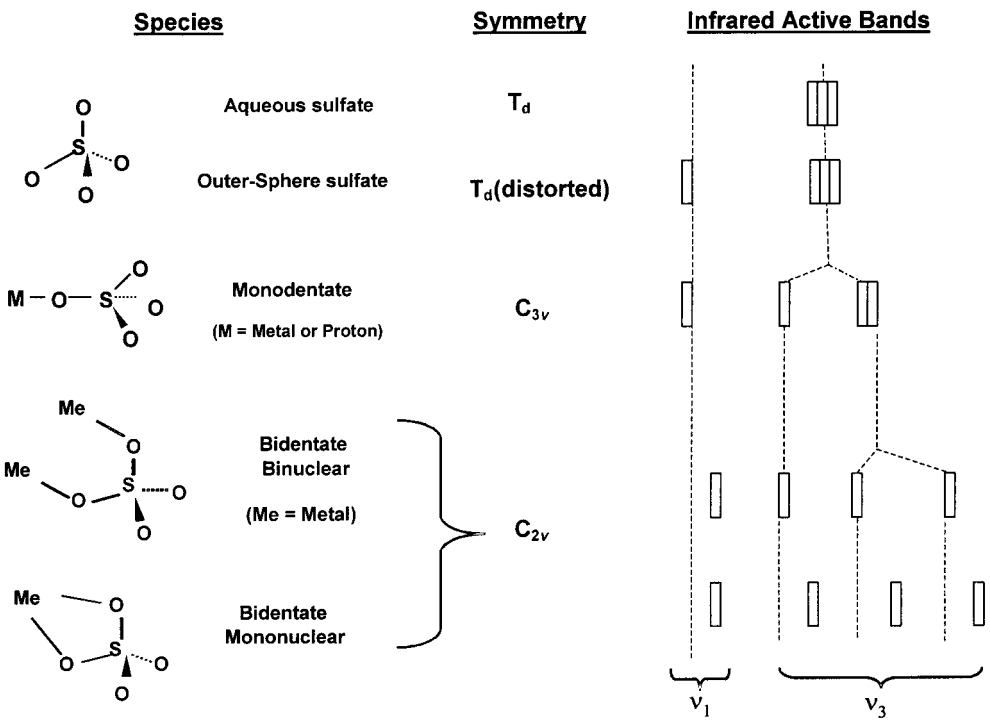

FIG. 1. The relationship between the molecular symmetry of sulfate complexes and the observed infrared spectrum they produce. Adapted from Hug (15).

MATERIALS AND METHODS

All FTIR experiments were conducted using a Perkin-Elmer 1720x spectrometer equipped with a purge gas generator and either a DTGS or MCT detector. A horizontal ATR accessory and flow cell (Spectra-Tech) as well as a Perkin-Elmer diffuse reflectance (DRIFT) accessory were used for sampling. Spectra were the result of 1000 co-added scans at a resolution of 4 cm^{-1} unless otherwise noted. All chemicals used were reagent grade.

Goethite Synthesis

The goethite used in this study was synthesized using the method of Schwertmann *et al.* (18). Initially, ferrihydrite was precipitated by adding 50 ml of 1 M ferric nitrate solution to 450 ml of 1 M KOH. This suspension of amorphous hydrous ferric oxide was then aged for 14 days at 25°C. The suspension was next washed via centrifugation, replacing the supernatant with doubly deionized water to remove residual KOH. The rinsed solid was then resuspended in 0.4 M HCl and shaken for 2 h using a mechanical shaker. This treatment was used to remove any remaining ferrihydrite from the surface of the goethite. The acidified goethite suspension was again washed via centrifugation to remove both HCl and dissolved iron. Finally, the goethite was dialyzed, frozen with liquid nitrogen, and freeze-dried. The solid was confirmed as goethite via infrared spectroscopy using both ATR and transmission mode KBr pellets. The external surface area determined from N_2 BET was 63.5 $m^2\ g^{-1}$ and the point of zero salt effect was 8.4, as determined via potentiometric titration in 0.1, 0.01, and 0.005 M sodium perchlorate.

Schwertmannite Synthesis

Schwertmannite, a poorly crystalline iron(III) oxy-hydroxy-sulfate was synthesized following the procedure of Schwertmann and Cornell (16). This mineral phase has approximately 10% by weight sulfate incorporated into its structure (1). Both the color and the infrared spectra of the synthesized product were consistent with schwertmannite. Infrared spectra of the schwertmannite were collected in ATR mode by mixing approximately 10 mg of solid with 500 μl of water, depositing the slurry onto the crystal, and collecting a spectrum once the solid had dried. Another sample was diluted to a concentration of 2.5% solid by weight using infrared grade KBr and run in diffuse reflectance mode.

In Situ FTIR Spectroscopy

Goethite was evenly deposited onto a 45° ZnSe ATR crystal using a variation of the technique described by Hug (19, 15). First, 500 μl of 0.01 M NaCl adjusted to pH 4.5 was pipetted onto the crystal, forming a large droplet. Then, 10 μl of a 250 g L^{-1} goethite suspension was placed into the center of the droplet with a pipette. The suspension was then mixed and spread evenly across the surface of the crystal using the pipette tip and allowed to dry. Once the deposit was dried, it was rinsed by holding it at an angle, placing a large drop of 0.01 M NaCl onto one edge, and allowing the droplet to slowly move across the deposit. At the end the excess electrolyte was absorbed with a KimWipe. Once the rinsed ATR crystal air-dried, it was placed into the flow cell. To determine the amount of goethite deposited on the ATR crystal, the crystal was weighed before and after deposition. In all cases, the difference was between 2.8 and 3.0 mg, which is in reasonable agreement with the theoretical value of 2.5 mg if all the goethite that is added forms a deposit.

The cell was then connected via tygon tubing to a 500-ml polypropylene reaction vessel that contained 400 ml of background electrolyte. NaCl was used as a background electrolyte due to the absence of absorbance in the mid-IR range. The vessel was N_2 purged and a combination pH electrode was used to monitor solution pH throughout the experiment. A stir bar and magnetic stir plate provided thorough mixing, and a small port was used to adjust pH with 0.1 M NaOH or 0.1 M HCl as needed and also to add 0.1 M Na_2SO_4. A diagram of the experimental apparatus is shown in Fig. 2. This experimental apparatus allows for direct and *in situ* measurements of both pH envelopes and adsorption isotherms of sulfate on goethite. The background electrolyte was circulated through the flow cell until there was no noticeable change in the ratio of successive spectra. At this time, a background spectrum was collected consisting of the absorbance of the ZnSe crystal and the deposited goethite. The remaining spectra were collected as a ratio to this background. Spectra were collected for 15 min prior to reactant addition to verify that no further changes of the background were occurring.

pH Envelopes

To generate pH envelopes, the outflow tube from the flow cell was connected to the reaction vessel containing 400 ml of background electrolyte solution at pH 9.0. Ionic strengths ranging from 0.1 to 0.005 M were used. Once a stable background was collected, 20 μM sulfate was added, and spectra were collected every 10 min. When there was no increase in the intensity of the spectra with time, it was assumed that an equilibrium state had been reached. At this point the pH was lowered 0.5 pH units by addition of 0.1 M HCl. This procedure was repeated down to pH 3.5.

Adsorption Isotherms

For the sulfate adsorption isotherms, the effluent from the flow cell was collected as waste instead of being circulated back to the reaction vessel. This was done to ensure that the equilibrium sulfate concentration (C_{eq}) could be determined. When the sulfate initially enters the flow cell, it is rapidly adsorbed to the deposited goethite in the flow cell and the sulfate concentration in the effluent will remain low. As the

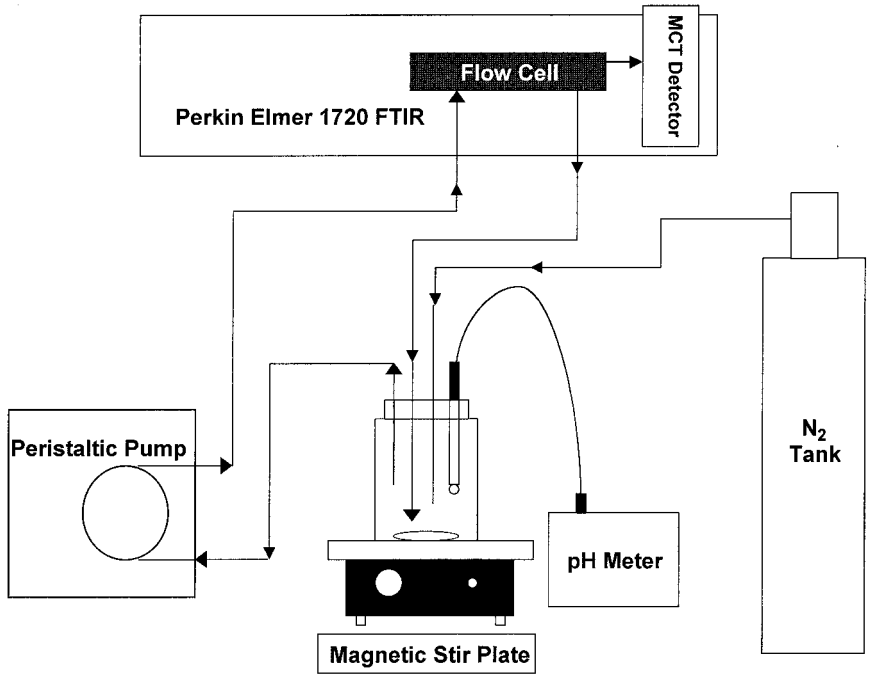

FIG. 2. Diagram depicting the experimental apparatus used for pH envelopes and adsorption isotherms.

system approaches equilibrium, however, the effluent concentration will rise until it equals the influent concentration. At this time the influent concentration is equal to C_{eq} and the system is at equilibrium.

For these experiments, equilibrium was defined as the point where no further increase in the infrared spectra arising from adsorbed sulfate was observed. The amount of stock 0.1 M Na_2SO_4 needed to adjust the remaining volume to the next sulfate concentration was calculated from the flow rate and the time elapsed since the pump was started. The sulfate concentration in the reaction vessel was then raised and allowed to reach a new equilibrium with the goethite in the flow cell. This is repeated to generate spectra of adsorbed sulfate as a function of equilibrium sulfate concentration. The integrated absorbance of these samples was plotted vs C_{eq}.

RESULTS

The results for a pH envelope experiment are shown in Fig. 3. The experiment was run in 0.01 M NaCl at a total sulfate concentration of 20 μM. The spectra are the result of 128 co-added scans at 4-cm^{-1} resolution. The experiment was initiated at pH 9.0, which is above the point of zero charge of the goethite used. At this pH, there should be very little adsorption of sulfate, as demonstrated by the extremely low absorbance of 0.002. This is the maximum absorbance that can be attributed to aqueous sulfate in this set of experimental data; greater absorbance values are due to the accumulation of sulfate at the goethite/aqueous interface. As the pH is lowered,

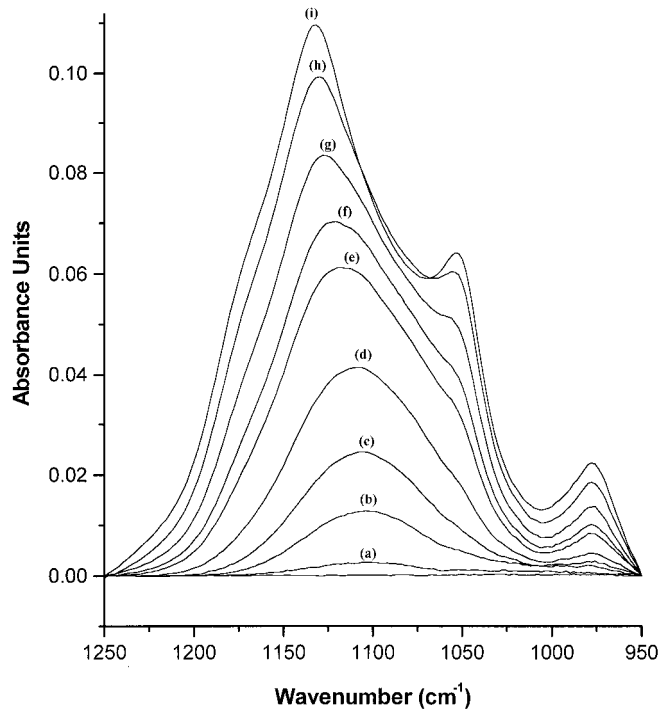

FIG. 3. Spectra from a pH envelope of sulfate adsorbed on goethite. Reaction conditions were 0.01 N NaCl and 20 μM SO_4^{2-}. The spectra were the result of 128 co-added scans at 4-cm^{-1} resolution. The spectra were collected at pH (from bottom): (a) 9.0, (b) 7.0, (c) 6.0, (d) 5.5, (e) 5.25, (f) 5.0, (g) 4.5, (h) 4.0, and (i) 3.5.

the absorbance increases, but the spectra remains very similar to aqueous sulfate, with the only visible peak (the ν_3 band) occurring at 1104 cm^{-1}. This ν_3 peak systematically shifts toward higher wavenumber, and the ν_1 band at 975 cm^{-1} becomes visible around pH 7. This is consistent with an outer-sphere surface complex formation since the degree of distortion of the tetrahedral symmetry should be directly related to the strength of the electrical field (in this case the surface charge, σ_0). This can explain the observed spectrum very well from pH 9 down to pH 6. Below pH 6, however, the ν_1 band becomes more sharply defined at 976 cm^{-1}. The ν_3 band also begins to split into two distinctive peaks at 1055 and 1133 cm^{-1} and a shoulder at 1170 cm^{-1}. This splitting indicates the presence of an inner-sphere sulfate surface complex, but detailed spectral analysis was necessary to determine the importance of the shoulder to the spectrum.

To verify that the spectral features attributed to inner-sphere sulfate surface complexes were not experimental artifacts caused by adjusting pH, and to obtain spectra with greater amounts of adsorbed sulfate, an adsorption isotherm was also conducted at pH 3.5. The spectra due to adsorbed sulfate obtained from an adsorption isotherm conducted at 0.01 M NaCl and pH 3.5 are shown in Fig. 4. It is notable that as the adsorbed sulfate increases, there is no change in the position of the peaks that appear in the spectra. This is indicative that the same types of surface complexes occur over a wide range of equilibrium concentrations (5–500 μM). Also of importance is that a peak at 992 cm^{-1} attributed to the ν_1 band of inner-sphere sulfate and used to fit the spectra from the pH envelope becomes plainly visible in the raw spectra (denoted by arrow) as the concentration increases.

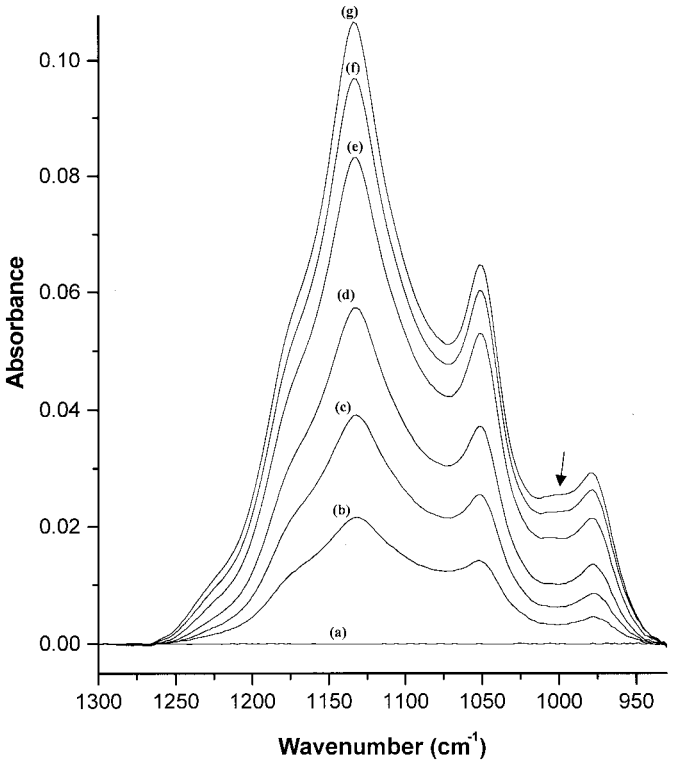

FIG. 4. Spectra from a sulfate adsorption isotherm conducted at pH 3.5 and $I = 0.01$. The spectra are the result of (from bottom) (a) 0, (b) 5, (c) 10, (d) 25, (e) 100, (f) 250, and (g) 500 μM equilibrium sulfate concentration. The arrow denotes the feature arising from a ν_1 peak at 992 cm^{-1}.

A spectral peak-fitting program (Peak Solve, Galactic Industries) was employed to fit peaks to the spectra and determine the symmetry of the surface complexes. A linear baseline was applied to all the spectra so the absorbance at 950 and 1250 cm^{-1} was equal to zero, and Gaussian functions were used for all peaks. Although infrared spectra are most commonly fit with Lorentzian functions, attempts to fit the inner-sphere complexes with Lorentzian functions were unsuccessful. Myneni and co-workers (20) also found that Gaussian peaks best fit the sulfate ν_3 bands of ettringite, a sulfate-bearing mineral. It was impossible to fit the spectra where inner-sphere complexes were present without also including the peaks at 1108 and 975 cm^{-1}, which are attributed to an outer-sphere complex. Once these peaks were included, it was determined that a second inner-sphere surface complex was also present. For this surface complex, the ν_3 band was split into three peaks at 1170, 1133, and 1055 cm^{-1} while another ν_1 band of lesser intensity than the ν_3 bands at 992 cm^{-1} also improved the fit. All the spectra from pH 3.5 to pH 5.0 could successfully be fit by fixing the position of the four peaks attributed to the inner-sphere complex, while allowing the position of the peaks assigned to outer-sphere sulfate to vary by $\pm$ 1 cm^{-1} between successive spectra. This variation was allowed since the increasingly positive surface charge of goethite as the pH is lowered could result in changes in distortion of the outer-sphere spectra. Figure 5a shows the fit of the pH 3.5 spectrum, while Fig. 5b demonstrates that the pH 5 spectrum could be fit equally well with the same peaks, although the relative contribution from the outer-sphere complex is greater at pH 5.0. The relative intensity of the observed inner-sphere peaks at 1170, 1133, 1051, and 992 cm^{-1} is approximately 0.6:1:0.6:0.2, respectively. These four peak positions and their relative intensities are consistent with a bidentate binuclear surface complex of either C_{2v} or possibly C_1 symmetry. This is because a monodentate surface complex would have only two peaks in the 1050 to 1200-cm^{-1} region and a bidentate mononuclear (chelating) surface complex would result in shifting of the three ν_3 peaks to wavenumbers much higher than is observed. It is also possible that while the results of the *in situ* experimentation reveal a bidentate binuclear configuration with respect to sulfate, they do not explicitly identify the ions which sulfate is bridging. This is due to the fact that the ν_3 band is fully active in the bidentate binuclear (C_{2v}) case and further lowering of the molecular symmetry (C_1) will not result in any further splitting of the ν_3 bands. While sulfate could be bridging two iron atoms, it is also possible that either bisulfate (HSO_4^-) or sodium sulfate ($NaSO_4^-$) is coordinated in a monodentate fashion to the iron oxide surface since complexes of a

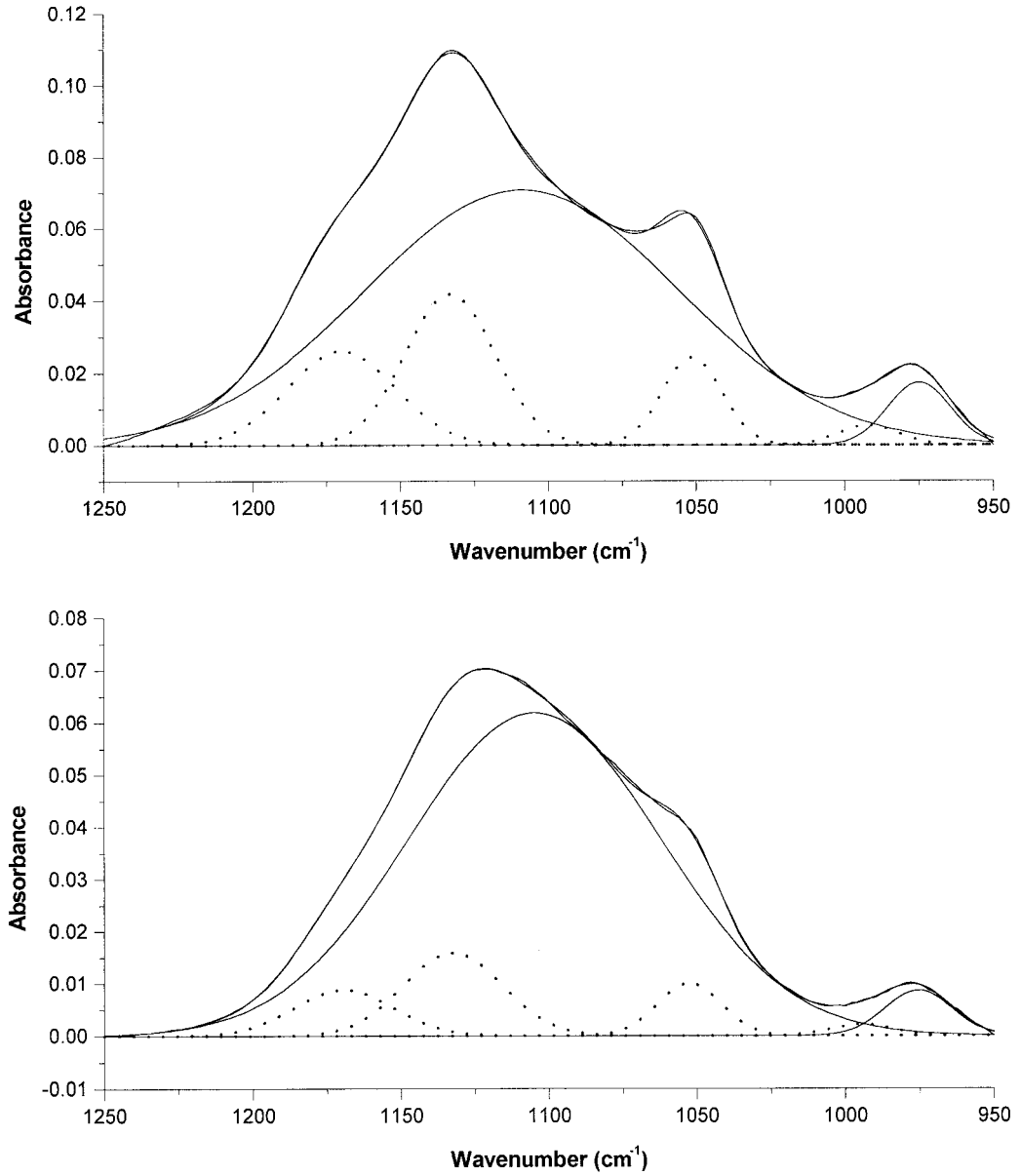

FIG. 5. (a) Fit of the pH 3.5 spectrum from the pH envelope shown in Fig. 3. The dotted lines denote the peaks arising from an inner-sphere complex. (b) Fit of the pH 5.0 spectrum from the pH envelope in Fig. 3. The peak positions used to fit the pH 3.5 spectrum were held constant for the fitting of this spectrum.

C_1 symmetry would also have three IR active ν_3 bands. Additionally, it is possible that the feature at 1170 cm^{-1} is the result of a hydrogen bond between an oxygen atom of a monodentate sulfate and an adjacent surface site. All these possibilities could result in the observed spectrum and are summarized in Fig. 6. It is noteworthy that the spectrum of inner-sphere sulfate adsorbed on goethite is extremely similar to the spectrum reported by Hug for $Fe(III)SO_{4\,(aq)}^{+}$ at pH 2.2 (15). The shoulder in Hug's work (15) was attributed to hydrogen-bonding interactions between sulfate and adjacent waters of the iron hydration shell. Since Fe(III) was present in excess of sulfate in that solution (18 mM Fe vs 10 mM SO_4^{2-}), it is also possible that some aqueous Fe_2SO_4 was present. An iron(III) bisulfate complex ($Fe–HSO_{4\,(aq)}^{2+}$) could also potentially explain the observed feature at 1185 cm^{-1} in Hug's (15) sample.

While these possibilities reinforce the proposed surface complexes, they can not be used to assign the observed sulfate bands with any certainty. To refine the surface complexation mechanism further, an adsorption experiment was conducted using D_2O as a solvent rather than H_2O. Spectra from sulfate adsorption experiments conducted at $I = 0.05$, pH 3.5, 100 μM sulfate, and either D_2O or H_2O as a solvent are shown in Fig. 7.

It is clear from Fig. 7 that there is a shift that occurs in the

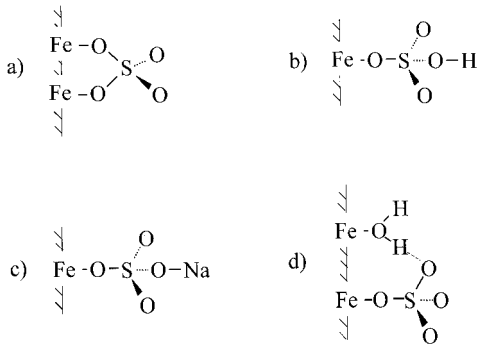

FIG. 6. Sulfate inner-sphere surface complexes that could possibly result in the experimentally observed spectral features. The drawings represent a bidentate complex bridging (a) two Fe atoms, (b) one Fe atom and one proton, (c) one Fe atom and one Na atom, and (d) a monodentate Fe-SO_4^- hydrogen bonded to an adjacent positively charged surface group.

ν_3 bands of sulfate adsorbed on goethite when D_2O is used as a solvent. Peaks occurring at 1133 and 1051 cm^{-1} in H_2O (splitting of the ν_3 band due to inner-sphere complexation) are both shifted approximately 8 cm^{-1} to 1125 and 1043 cm^{-1} in D_2O. This shift to lower wavenumber is characteristic for substitution of a deuterium ion for a proton in a molecular complex. Since these peaks are the result of inner-sphere complexation, it is therefore reasonable to conclude that a proton is present in the inner-sphere surface complex. On this basis, both bidentate bridging (=Fe_2SO4) and monodentate sodium sulfate surface complexes can be ruled out as the source of the observed spectra. The only possible surface complexes which would involve a proton are bisulfate sorbed as a monodentate complex (Fig. 6b) or monodentate sulfate that is hydrogen bonded to an adjacent surface site (Fig. 6d).

In Fig. 8, the effect of ionic strength on the mechanism of sulfate adsorption is illustrated. Since the amount of goethite varies between experiments, the spectra were normalized to the maximum absorbance to compare their spectra. As expected, increasing ionic strength results in less outer-sphere adsorption. This can be seen by the increasing importance of the inner-sphere peaks to the overall spectra in the higher ionic strength spectra (b). The earlier assignment of the peaks at 1110 and 976 cm^{-1} to outer-sphere sulfate is also supported by these results, since the relative importance of these peaks is greater in lower ionic strength spectra (a) where there is more outer-sphere adsorption. The assignment of the peak at 976 cm^{-1} to the ν_1 band of outer-sphere sulfate is also supported by the observation that the ratio of the outer-sphere peak areas is 0.04:1.00 in both spectra.

As a reference for sulfate coordination, infrared spectra of schwertmannite were collected. Figure 9 shows the absorbance of schwertmannite in the region from 1250 to 950 cm^{-1}, which includes all the peaks due to splitting of the ν_1 and ν_3 bands. DRIFT (a) and ATR deposition (c) techniques were used to determine the impact of sample preparation on the infrared spectra. ATR-FTIR spectra of 20 μM sulfate adsorbed on

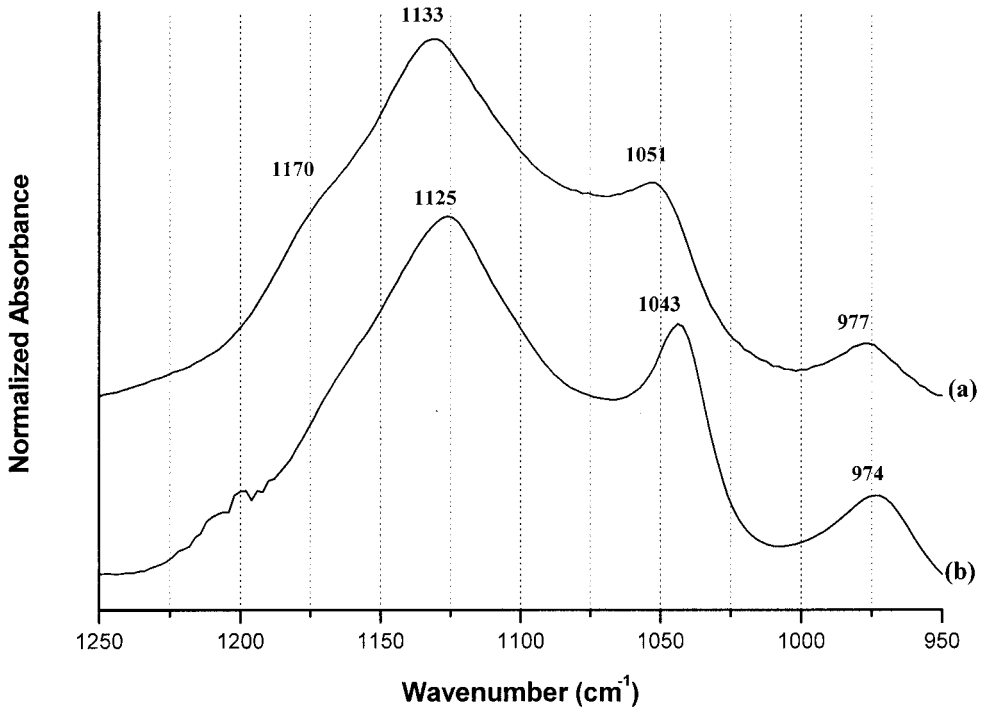

FIG. 7. Comparison of spectra of adsorbed sulfate collected in (a) H_2O and (b) D_2O. In both cases the reaction conditions were pH 3.5, $I = 0.05$, and an initial sulfate concentration of 100 μM.

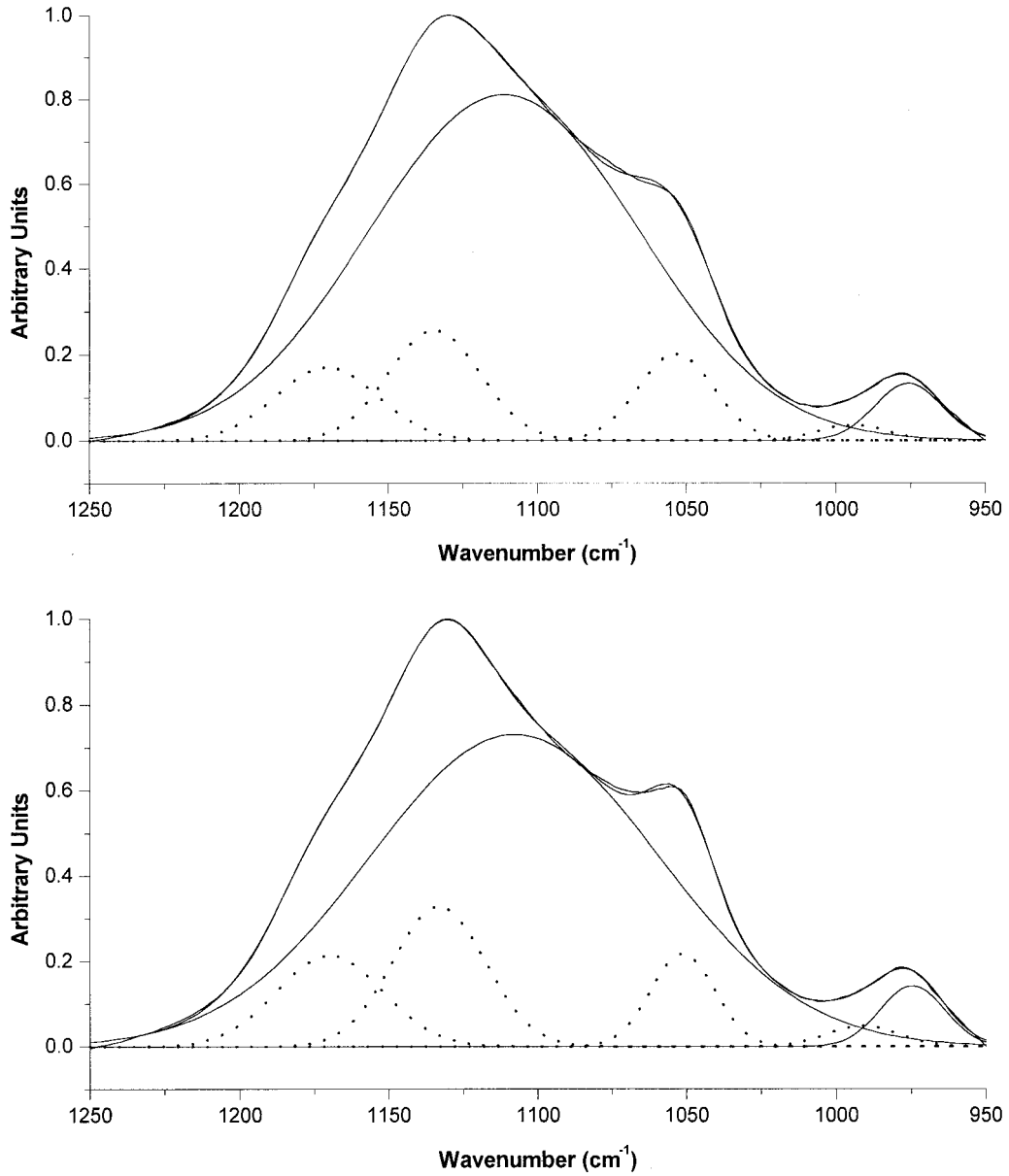

FIG. 8. Variation of spectra of adsorbed sulfate with ionic strength. In both cases the reaction conditions were pH 4.00 and 20 μM SO_4^{2-} added. Spectrum (a) was collected at ionic strength 0.005, while (b) was collected at $I = 0.1$.

goethite at pH 3.5 (b) and pH 5.0 (d) from the pH envelope are shown for comparison with the schwertmannite peaks. In both schwertmannite sample preparations it is evident that splitting of the v_3 band of sulfate occurs. In the case of the DRIFT spectrum there is a split into three peaks at 1050, 1130, and 1208 cm^{-1}. This indicates that sulfate exists in a bidentate coordination which is in agreement with the results of Bigham *et al.* (1). With the exception of the peak at 1208 cm^{-1} (to be discussed later), the agreement between the peaks of sulfate adsorbed onto goethite at pH 3.5 with those for the schwertmannite DRIFT spectrum are quite good. In both spectra there is well-defined splitting of the sulfate v_3 bands that is diagnostic for inner-sphere complexation.

There are, however, noticeable differences between the spectrum of schwertmannite deposited onto the ATR crystal and the DRIFT spectrum. The broadening of the spectra in the region from 1140 to 1075 cm^{-1} is due to the presence of two peaks. The good agreement between one of these peaks and that of aqueous sulfate (e) suggests that there is an additional component to the spectra that has symmetry very similar to free sulfate. Since the sample had been extensively dialyzed and freeze-dried prior to experimentation, this peak is most likely

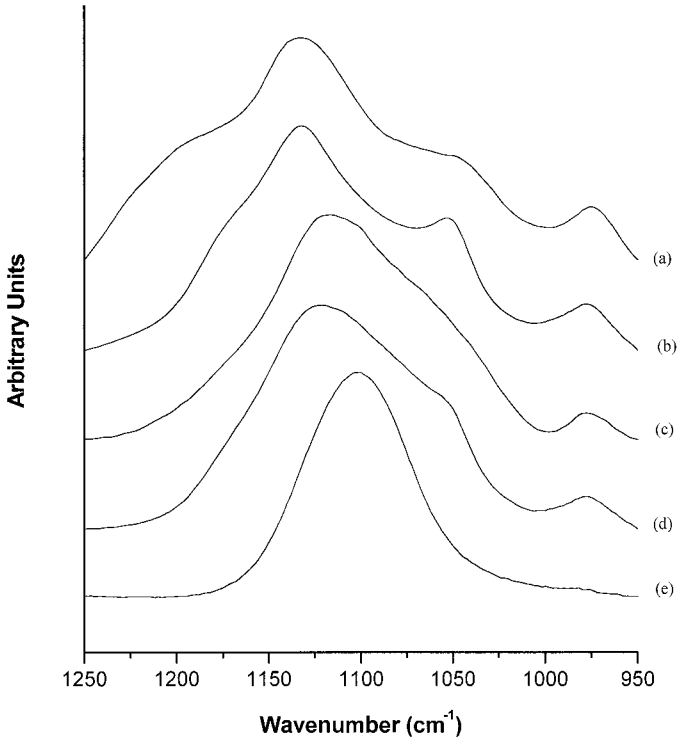

FIG. 9. Comparison of schwertmannite spectrum collected via DRIFT (a) and ATR (c) to the ATR spectrum of 20 μM sulfate adsorbed on goethite at pH 3.5 (b) and pH 5.0 (d) and 100 mM aqueous sulfate (e).

due to an outer-sphere sulfate complex and not due to the presence of residual aqueous sulfate in the sample. These findings are consistent with the proposed structure of schwertmannite (1), which includes sulfate as a counterion in internal channels similar to chloride in akaganeite. Dilution with KBr removes this feature from the sample, most likely due to displacement of outer-sphere sulfate with bromide in the channels and the formation of K_2SO_4 salt. Since the schwertmannite sample had been freeze-dried prior to dilution in KBr, it is also possible that removal of surface water favored a conversion from outer-sphere to inner-sphere surface complexes. The broadening of the peaks of the DRIFT schwertmannite sample compared to those of adsorbed sulfate at pH 3.5 also implies less order in the sulfate-bonding environment of schwertmannite. This could either be due to the amorphous nature of the solid or possibly to K_2SO_4 formation in the DRIFT sample. Both K_2SO_4 and bidentate binuclear Fe_2SO_4 have C_{2v} symmetry but different substituent cations would result in varying degrees of splitting of the ν_3 band. The peak at 1208 cm^{-1} also disappears in the ATR sample. Hug (15) noted the appearance of a peak at 1200 cm^{-1} upon drying sulfate solutions adsorbed on hematite. It is therefore likely that this peak is an artifact of sample preparation. The excellent agreement between the *in situ* schwertmannite ATR deposit and sulfate adsorbed on goethite at pH 5.0 indicates a similar bonding environment in both cases. However, an exact assignment of symmetry for the inner-sphere complex of schwertmannite is difficult without conducting D_2O experiments similar to those done with adsorbed sulfate on goethite. These experiments were unsuccessful (data not shown), due to the need to thoroughly dry the deposited schwertmannite to avoid interference from D_2O. While the results were very similar to the DRIFT spectra of schwertmannite in Fig. 9a, it is questionable to draw conclusions based on such *ex situ* experiments.

DISCUSSION

We observe a continuum of inner-sphere and outer-sphere sulfate complexation on goethite. Inner-sphere sulfate adsorption on iron oxides increases as the pH is lowered, and outer-sphere adsorption increases as ionic strength is decreased. This adsorption behavior can be readily explained by the concept of ligand exchange. In basic conditions, the singly coordinated surface hydroxyls of metal oxides exist as either $Me–O^-$ or as Me–OH functional groups. The bonds between the oxygen ligands and the metal center tend to be strong, and ligand exchange is less favorable since the hydroxide ligands are difficult to displace and are also present in higher concentrations in solution than is a trace adsorbate such as sulfate. As pH decreases, singly coordinated hydroxyls (Fe–OH) protonate to produce $Fe–OH_2^+$ functional groups. The water attached to the iron(III) is a weak ligand with high lability and can more easily be displaced by a competing ligand such as sulfate, forming an inner-sphere surface complex. To fully understand the reactivity of sulfate with goethite, and to explain differences in sulfate adsorption on hematite and goethite, a detailed understanding of the surface-charging behavior of both iron oxides is required.

It is noteworthy that sulfate only forms inner-sphere monodentate surface complexes on hematite in aqueous solution (15) while forming a mixture of outer-sphere and inner-sphere complexes on goethite. Since both the goethite used in this experiment and the hematite used by Hug (13) had a PZC between 8 and 8.5, and in both cases the reactive site is probably $Fe–OH_2^+$, it is somewhat surprising that their reactivities are so markedly different. Differences apparently exist between the population of functional groups at the metal oxide surface that can account for the different sulfate adsorption behavior observed in the two systems. Researchers (21) have successfully applied a multisite complexation (MUSIC) approach to determine the relative site densities and log K values for all functional groups present on various crystal faces for both goethite and hematite. The results of this analysis can provide valuable insight into the observed adsorption behavior of sulfate and are used as a point of reference for the discussion that follows.

On goethite, the 110 crystal face is dominant, and the sites that readily protonate are the singly coordinated (Fe–O) and about 67% of the triply coordinated (Fe_3O) surface groups. At the PZC (around 9.0) the singly coordinated surface groups

exist as Fe–OH due to the extremely high log K, and the Fe_3O sites are ~70% Fe_3OH. As the pH is lowered from the point of zero charge, only the Fe_3O sites protonate until about pH 7. This explains the observed outer-sphere complexation because this protonation increases the positive charge on goethite (Fe_3OH has $+\frac{1}{2}$ formal charge) and therefore increases sulfate adsorption. However, no $FeOH_2^+$ sites necessary for inner-sphere sulfate complexation appear until the pH is lowered further.

With hematite, the surface functional groups behave somewhat differently. The 110 and the 001 faces predominate. Since the 001 crystal face has a PZC close to that of the hematite used by Hug (15), this crystal face likely contributed more to the results of Hug's (15) experiments than the 110 face with its PZC of 11. It has also been determined that sulfate forms bidentate binuclear surface complexes on most crystal faces, and monodentate surface complexes only on the 001 planes (22). On the 001 face, surface functional groups occur due to imperfections in the crystal structure. Both Fe–O and Fe_2O functional groups exist. At the PZC, approximately 80% of the singly coordinated sites exist as $Fe–OH_2^+$, which are capable of ligand substitution reactions with oxyanions. As pH is decreased below the PZC, the remainder of the Fe–OH sites protonate and the Fe_2O^- sites protonate to form the neutral Fe_2OH. Since the reactive surface sites are formed at a much higher pH on hematite and protonation of the Fe_2O sites does not promote outer-sphere adsorption, inner-sphere surface complexes are more favorable. This can explain Hug's observation (15) that sulfate forms primarily inner-sphere surface complexes over all pH values on hematite.

A final point for discussion is the identity of the inner-sphere surface complex that occurs on goethite. Two possibilities seem likely: bisulfate sorbed as a monodentate complex as in Fig. 6b or monodentate sulfate that is hydrogen bonded to an adjacent surface site as in Fig. 6d. It is difficult to distinguish between these two complexes based on the spectra alone, but two observations favor the formation of monodentate bisulfate surface complexes. First of all, there is the continued increase in adsorption that occurs as pH is lowered below 4.0. In fact, sulfate adsorption continues to increase until the pK_{a2} (~1.9) is reached, although spectroscopic experiments were not conducted below pH 3.5 due to limitations of the ZnSe crystal. The surface functional groups should be fully protonated even at pH 4.0, so site availability should be fairly constant. As pH is lowered, the concentration of sulfate actually decreases since bisulfate becomes a larger component of the aqueous equilibrium. This should be reflected in a decrease in the amount of sulfate adsorbed if monodentate sulfate with hydrogen bonding is responsible for the spectral features. A second argument can be made based on the results of the adsorption isotherm from Fig. 4. If monodentate sulfate forming hydrogen bonds with adjacent surface sites is the dominant mechanism, then one would expect the spectra to become more similar to monodentate sulfate as the surface loading increased. This is due to the fact that as the system approaches monolayer coverage, there would be fewer sites remaining for hydrogen bonding. Since both the shoulder at 1170 cm^{-1} and the feature at 992 cm^{-1} continue to be visible, one can infer that bisulfate is the active surface species.

The possibility of an inner-sphere bisulfate surface complex can also be supported by the results of other researchers. Persson and Lövgren (13) predicted the presence of a bisulfate–goethite complex to occur below pH 5.0 based on the potentiometric titrations of sulfate–goethite suspensions. While they assigned an outer-sphere mechanism to the bisulfate complex, this was based on DRIFT spectroscopy with considerable sample modification. Additionally, Sparks and Zhang (7) noted that sulfate adsorption was accompanied by simultaneous proton uptake. This is also in reasonable agreement with an inner-sphere bisulfate complex since adsorption of bisulfate would result in additional bisulfate production in solution at a constant pH to maintain equilibrium. The surface charge of goethite would also be lowered somewhat by bisulfate adsorption (from $>Fe–OH_2^+$ to $>Fe–HSO_4$) so that protons could also be adsorbed elsewhere on the goethite surface.

As mentioned earlier, our spectroscopic findings seem quite different from the DRIFT results of Persson and Lövgren (13), which indicated that sulfate adsorbs to goethite as an outer-sphere complex regardless of pH or ionic strength. It is important, however, to note the differences in experimental technique. In the studies of Persson and Lövgren (13), samples were diluted in KBr. Since the samples were not subjected to high temperature or freeze-drying, it is probable that surface water remained present. Dilution in KBr would then result in the sample pH shifting to a value similar to that of saturated KBr (approximately pH 6). This recently has been shown to occur by researchers investigating the effect of hematite morphology on sulfate adsorption (22). It has been noted in Hug's work (15) and also observed in this study that sulfate adsorption is quite sensitive to changes in pH, and the shift in pH due to dilution in KBr would likely result in a rapid change of the sulfate surface complex. This explains the observed outer-sphere complexation of sulfate in DRIFT samples since at pH 6 the spectrum is dominated by outer-sphere adsorption (Fig. 3). The peaks diagnostic for an inner-sphere complex of C_{2v} or C_1 symmetry are also seen in the DRIFT spectrum of Persson and Lövgren (13), but they are much lower in intensity than the peaks attributed to inner-sphere sulfate surface complexes in our research.

It is easier to reconcile these results with the findings of Parfitt and Smart (11), who used dried samples diluted with KBr and pressed into disks. They determined that sulfate forms inner-sphere bidentate binuclear surface complexes on goethite. The differences between these results and *in situ* experimentation are analogous to the differences between the DRIFT and ATR schwertmannite samples (Figure 7a and 7c). Sample drying strongly favors the inner-sphere complex and additionally shifts one of the v_3 peaks from 1170 to 1200 cm^{-1}.

CONCLUSIONS

While FTIR spectroscopy is a powerful analytical tool with the potential to conclusively determine the mechanism of adsorption of a variety of environmentally important oxyanions, care must be taken in experimental preparation. Drying and dilution in KBr can significantly alter the spectra of samples and can therefore lead to incorrect conclusions about the bonding environment of adsorbates. Aqueous schwertmannite suspensions contain considerably more sulfate bound in an outer-sphere coordination than previously reported with dried samples in KBr. The continuum between outer- and inner-sphere sulfate complexes can only be observed *in situ.*

Sulfate adsorption on goethite occurs via both outer-sphere and inner-sphere complexation. The relative importance of both complexes is a function of both pH and ionic strength, with outer-sphere adsorption dominating with increasing pH and decreasing ionic strength. Inner-sphere adsorption becomes more important with decreasing pH and increasing ionic strength. This pH-dependent formation of an inner-sphere sulfate surface complex can be explained by the availability of $Fe–OH_2^+$ sites at the goethite surface. The inner-sphere sulfate complex is either a monodentate bisulfate surface complex or a monodentate sulfate surface complex with hydrogen bonding to an adjacent surface site. Although aqueous bisulfate concentrations are negligible at pH 4 and above, it apparently has a much higher affinity for the goethite surface than does sulfate. This indicates that the speciation of sulfate at the goethite/water interface can be markedly different from the speciation in bulk solution. The spectrum of sulfate adsorbed on goethite at pH 5 is very similar to that of schwertmannite collected *in situ*, where sulfate also exists as both outer-sphere and inner-sphere complexes.

ACKNOWLEDGMENTS

The authors thank Hotze Wijnja (University of Connecticut) for discussion and helpful comments relating to the interpretation of the infrared spectra and Eef Elzinga (University of Delaware) for his careful review of this work and helpful suggestions.

REFERENCES

1. Bigham, J. M., Schwertmann, U., Carlson, L., and Murad, E., *Geochim. Cosmochim. Acta* **54,** 2743 (1990).
2. Ali, M. A., and Dzombak, D. A., *Geochim. Cosmochim. Acta* **60,** 5045 (1996).
3. Bleam, W. F., and Weesner, F. J., *J. Colloid Interface Sci.* **205,** 380 (1998).
4. Geelhoed, J. S., Hiemstra, T., and van Riemsdijk, W.H., *Geochim. Cosmochim. Acta* **61,** 2389 (1997).
5. Ali, M. A., and Dzombak, D. A., *Environ. Sci. Technol.* **30,** 1061 (1996).
6. Charlet, L., Dise, N., and Stumm, W., *Agr. Ecosyst.Environ.* **47,** 87 (1993).
7. Zhang, P. C., and Sparks, D. L., *Soil Sci. Soc. Am. J.* **54,** 1266 (1990).
8. Sposito, G. A., "The Surface Chemistry of Soils." Oxford University Press, New York, 1984.
9. Yates, D. E., and Healy, T. W., *J. Colloid Interface Sci.* **52,** 222 (1975).
10. Sparks, D. L., "Environmental Soil Chemistry." Academic Press, San Diego, 1995.
11. Parfitt, R. L., and R. Smart, S. C., *Soil Sci. Soc. Am. J.* **42,** 48 (1978).
12. Turner, I. J., and Kramer, J. R., *Soil Sci.* **152,** 227 (1991).
13. Persson, P., and Lövgren, L., *Geochim. Cosmochim. Acta* **60,** 2789 (1996).
14. Eggleston, C. M., Hug, S., Stumm, W., Sulzberger, B., and dos Santos Alfonso, M., *Geochim. Cosmochim. Acta* **62,** 585 (1998).
15. Hug, S. J., *J. Colloid Interface Sci.* **188,** 415 (1997).
16. Schwertmann, U., and Cornell, R. M., "Iron Oxides in the Laboratory; Preparation and Characterization." Weinheim, New York, 1991.
17. Nakamoto, K., "Infrared and Raman Spectra of Inorganic and Coordination Compounds." Wiley, New York, 1986.
18. Schwertmann, U., Cambier, P., and Murad, E., *Clays Clay Miner.* **33,** 369 (1985).
19. Hug, S. J., and Sulzberger, B., *Langmuir* **10,** 3587 (1994).
20. Myneni, S. C. B., Traina, S. J., Waychunas, G. A., and Logan, T. J., *Geochim. Cosmochim. Acta* **62,** 3499 (1998).
21. Venema, P., Hiemstra, T., Weidler, P. G., van Riemsdijk, W. H., *J. Colloid Interface Sci.* **198,** 282 (1998).
22. Sugimoto, T., and Wang, Y., *J. Colloid Interface Sci.* **207,** 137 (1998).